ISSN 1674-1056
http://cpb.iphy.ac.cn
http://iopscience.iop.org/cpb
中国物理 B
Chinese Physics
中国物理
Chinese Physics B

Phase-dependent double optomechanically induced transparency in a hybrid optomechanical cavity system with coherently mechanical driving

Shi-Chao Wu(吴士超), Li-Guo Qin(秦立国), Jian Lu(鹿建), Zhong-Yang Wang(王中阳)

Citation: Chin. Phys. B . 2019, 28(7): 074204. **doi:** 10.1088/1674-1056/28/7/074204
Journal homepage: http://cpb.iphy.ac.cn; http://iopscience.iop.org/cpb

What follows is a list of articles you may be interested in

Dynamic properties of atomic collective decay in cavity quantum electrodynamics

Yu-Feng Han(韩玉峰), Cheng-Jie Zhu(朱成杰), Xian-Shan Huang(黄仙山), Ya-Ping Yang(羊亚平)

Chin. Phys. B . 2018, 27(12): 124206. **doi:** 10.1088/1674-1056/27/12/124206

An analytical variational method for the biased quantum Rabi model in the ultra-strong coupling regime

Bin-Bin Mao(毛斌斌), Maoxin Liu(刘卯鑫), Wei Wu(吴威), Liangsheng Li(李粮生), Zu-Jian Ying(应祖建), Hong-Gang Luo(罗洪刚)

Chin. Phys. B . 2018, 27(5): 054219. **doi:** 10.1088/1674-1056/27/5/054219

Optomechanically induced transparency with Bose–Einstein condensate in double-cavity optomechanical system

Li-Wei Liu(刘利伟), Duo-Jie Gengzang(更藏多杰), Xiu-Jia An(安秀加), Pei-Yu Wang(王培煜)

Chin. Phys. B . 2018, 27(3): 034205. **doi:** 10.1088/1674-1056/27/3/034205

Controllable double electromagnetically induced transparency in a closed four-level-loop cavity–atom system

Miao-Di Guo(郭苗迪), Xue-Mei Su(苏雪梅)

Chin. Phys. B . 2017, 26(7): 074207. **doi:** 10.1088/1674-1056/26/7/074207

Triple optomechanical induced transparency in a two-cavity system

Shi-Chao Wu(吴士超), Li-Guo Qin(秦立国), Jun Jing(景俊), Guo-Hong Yang(杨国宏), Zhong-Yang Wang(王中阳)

Chin. Phys. B . 2016, 25(5): 054203. **doi:** 10.1088/1674-1056/25/5/054203

Phase-dependent double optomechanically induced transparency in a hybrid optomechanical cavity system with coherently mechanical driving*

Shi-Chao Wu(吴士超)[1,3], Li-Guo Qin(秦立国)[1,2,†], Jian Lu(鹿建)[1], and Zhong-Yang Wang(王中阳)[1,‡]

[1] *Shanghai Advanced Research Institute, Chinese Academy of Sciences, Shanghai* 201210, *China*
[2] *School of Mathematics, Physics and Statistics, Shanghai University Of Engineering Science, Shanghai* 201620, *China*
[3] *University of Chinese Academy of Sciences, Beijing* 100049, *China*

(Received 19 February 2019; revised manuscript received 12 April 2019; published online 31 May 2019)

We propose a scheme that can generate tunable double optomechanically induced transparency in a hybrid optomechanical cavity system. In this system, the mechanical resonator of the optomechanical cavity is coupled with an additional mechanical resonator and the additional mechanical resonator can be driven by a weak external coherently mechanical driving field. We show that both the intensity and the phase of the external mechanical driving field can control the propagation of the probe field, including changing the transmission spectrum from double windows to a single-window. Our study also provides an effective way to generate intensity-controllable, narrow-bandwidth transmission spectra, with the probe field modulated from excessive opacity to remarkable amplification.

Keywords: double optomechanically induced transparency, hybrid optomechanical cavity system, pump–probe spectroscopy, mechanical driving

PACS: 42.50.pq, 42.15.Eq, 42.62.Fi, 07.10.Cm **DOI:** 10.1088/1674-1056/28/7/074204

1. Introduction

Engineering and manipulating the interaction between the optical and mechanical modes is an active research area, which has been studied theoretically and experimentally in many systems,[1–15] such as optomechanical systems.[9–15] A traditional optomechanical system is composed of an optical cavity and a mechanical resonator. Following the development of micro- and nano-fabrication techniques, it is now feasible to integrate the traditional optomechanical system with other systems, such as additional mechanical resonators,[16,17] superconducting microwave cavities,[18] phononic[19] or photonic crystal cavities,[4] piezoelectric systems,[20] and charged systems.[21] Compared with the traditional optomechanical system, the photon–phonon interaction in these hybrid optomechanical systems can be controlled by the optical radiation pressure, piezoelectric forces,[4,5] Lorentz forces,[22,23] and Coulomb forces.[17,24] The interaction between the optical and mechanical modes can generate many interesting phenomena in the optomechanical systems, such as optomechanically induced transparency (OMIT). OMIT is a phenomenon in which a photon cavity can be changed from opacity to transparency. It arises from the quantum interference effect between different energy levels.[5,11,25–29] Similar to electromagnetically induced transparency (EIT) observed in three-level atomic systems,[30–33] OMIT can also be applied to many fields, including quantum ground-state cooling,[34,35] fast and slow light,[36,37] and quantum information processing.[38,39]

Compared with the traditional optomechanical system, in hybrid optomechanical systems the single-OMIT has been extended to the double-OMIT.[14,17,40–45] In contrast to the single-window transmission spectrum observed in the OMIT, the double-window transmission spectrum can be observed in the double-OMIT. This phenomenon is similar to the two-photon absorption observed in four-level energy-structure atomic systems.[46,47] In double-OMIT hybrid optomechanical systems, which combine a traditional optomechanical system with an additional two-level energy system, the original three-level energy system is converted into a four-level system. The double-OMIT is generated by quantum interference between the pathways of different energy levels. The double-OMIT has many applications, including optical switches,[45] temperature measurement,[24] high-resolution spectroscopy, and double-channel quantum information processing.[17,42]

In this study, we propose a hybrid optomechanical system in which the mechanical resonator of the optomechanical cavity is coupled with an additional mechanical resonator, and the additional mechanical resonator can be driven by a weak external coherently mechanical driving field. In this system, the tunable double-OMIT can be generated. We also show that both the intensity and the phase of the external coherently me-

*Project supported by the Strategic Priority Research Program of China (Grant No. XDB01010200), the National Natural Science Foundation of China (Grant Nos. 61605225, 11674337, and 11547035), and Natural Science Foundation of Shanghai, China (Grant No. 16ZR1448400).

†Corresponding author. E-mail: lgqin@foxmail.com
‡Corresponding author. E-mail: wangzy@sari.ac.cn

© 2019 Chinese Physical Society and IOP Publishing Ltd

chanical driving field can control the propagation of the probe field, including changing the transmission spectrum from double windows to single window.

The phenomenon of the tunable double-OMIT arises because the energy levels of the system can be modulated by the external mechanical driving field. In our system, a four-level energy structure can be formed. Under the coupling effect between the mechanical resonators, the energy level of the original mechanical resonator is dressed into an empty state. When the external driving field is applied to the additional mechanical resonator, the empty state level is replenished to yield an occupied state. Consequently, the absorption and the dispersion of the probe field are modulated by the interference of the optical pumped field and the external mechanical driving field.

Many devices can be applied to implement our scheme, both in theory and in experimentation. The two mechanical resonators can be coupled to each other via the common coupling overhang or Coulomb interaction.[40,48–54] More importantly, the strength of coupling between them can be modulated flexibly.[53,54] With regard to the mechanical driving field, many forms of driving forces can be applied. For example, the mechanical resonators can be driven by piezoelectric forces if they are fabricated with piezoelectric materials,[55–58] and by Lorentz forces where a current-carrying resonator is placed in the magnetic field.[22,23]

Hybrid optomechanical cavity systems with coherently mechanical driving have been studied in many fields, including the implementation of single[29,59,60] and double[13,14] optomechanically induced opacity and amplification, and weak force measurement.[61] Compared to these systems, our scheme has the following features: (i) it can realize switching between the double-OMIT and the single-OMIT, which can be controlled by many forms of mechanical driving fields, such as piezoelectric forces and Lorentz forces; and (ii) our scheme also provides an effective way to generate an intensity-controllable narrow-bandwidth transmission spectrum, with the probe field modulated from excessive opacity to remarkable amplification.

The remainder of this paper is organized as follows. In Section 2, we describe the theoretical model and derive the dynamical equation of the proposed system. In Section 3, we discuss the experimental feasibility and physical mechanism of the double-OMIT. In Section 4, the external mechanical driving field-controlled double-OMIT is presented. In Section 5, we discuss the tunable double-OMIT controlled by other parameters of the system. The last section offers the conclusions of this paper.

2. Theoretical model and dynamical equation

A schematic diagram of the proposed hybrid optomechanical cavity system is shown in Fig. 1, in which the mechanical resonator b of a traditional optomechanical cavity is coupled with an additional mechanical resonator c, and the additional mechanical resonator c is driven by a weak external coherently mechanical driving field. The frequency of the optical cavity is ω_a, and the frequencies of the two mechanical resonators are ω_b and ω_c, respectively. The mechanical resonators b and c can be coupled via the common coupling overhang or Coulomb interaction.[40,48–54] The mechanical driving field can be applied to the system in the form of piezoelectric forces[55–58] and Lorentz forces.[22,23] Consequently, the hybrid optomechanical cavity system can be driven by both the optical fields and the mechanical driving field. We assume that the optomechanical cavity is driven by a strong optical pump field with frequency $\omega_{\rm pu}$ and a weak optical probe field with frequency $\omega_{\rm pr}$. Mechanical resonator c is driven by a weak external coherently mechanical driving field with frequency ω_d. The strength of the optomechanical coupling between the optical fields and the mechanical resonator b is referred to as $G_{\rm om}$, and the coupling strength between the mechanical resonators b and c is referred to as J.

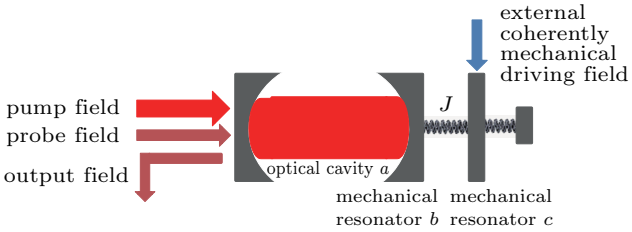


Fig. 1. Schematic diagram of the hybrid optomechanical system, in which the mechanical resonator b of a traditional optomechanical cavity is coupled with an additional mechanical resonator c, and the additional mechanical resonator c is driven by a weak external coherently mechanical driving field. The optomechanical cavity is driven by a strong optical pump field and a weak optical probe field. The coupling strength between the mechanical resonators is denoted by J.

In the frame rotating at the frequency of the pump field $\omega_{\rm pu}$, the Hamiltonian of the total system is given as

$$H = H_0 + H_{\rm I}, \tag{1}$$

where

$$\begin{aligned} H_0 &= \hbar\Delta_a \hat{a}^\dagger a + \hbar\omega_b \hat{b}^\dagger \hat{b} + \hbar\omega_c \hat{c}^\dagger \hat{c}, \qquad (2)\\ H_{\rm I} &= -\hbar g_{\rm om} \hat{a}^\dagger \hat{a}(\hat{b}^\dagger + \hat{b}) - \hbar J(\hat{b}^\dagger \hat{c} + \hat{b}\hat{c}^\dagger) \\ &\quad + (\mathrm{i}\hbar\varepsilon_{\rm pu}\hat{a}^\dagger + \mathrm{i}\hbar\varepsilon_{\rm pr}\mathrm{e}^{-\mathrm{i}\delta t - \mathrm{i}\phi_{\rm p}}\hat{a}^\dagger \\ &\quad + \mathrm{i}\hbar\varepsilon_d \mathrm{e}^{-\mathrm{i}\omega_d t - \mathrm{i}\phi_d}\hat{c}^\dagger + \mathrm{H.c.}). \qquad (3) \end{aligned}$$

Here, H_0 is the free Hamiltonian of the system, where $\hat{a}$, $\hat{b}$, and $\hat{c}$ are the annihilation operators of the optical cavity mode a, and the mechanical phonon modes b and c, respectively. $\Delta_a = \omega_a - \omega_{\rm pu}$ is the frequency detuning of the optical pump field from the optical cavity. $H_{\rm I}$ describes the interaction Hamiltonian. The first term is the optomechanical interaction term, $g_{\rm om} = (\omega_a/L)\sqrt{\hbar/m\omega_b}$ denotes the strength of single-photon optomechanical coupling between the optical

field mode and the mechanical phonon mode, where m is the effective mass of the mechanical mode and L is the effective length of the optical cavity. The second term describes the interaction between the coupling mechanical resonators b and c, where J is the coupling strength. The last four terms describe the energy of the input fields, and $\varepsilon_{\rm pu}=\sqrt{P_{\rm pu}\kappa_a/(\hbar\omega_{\rm pu})}$ and $\varepsilon_{\rm pr}=\sqrt{P_{\rm pr}\kappa_a/(\hbar\omega_{\rm pr})}$ are the amplitudes of the optical pump field and the probe field, respectively, where $P_{\rm pu}$ and $P_{\rm pr}$ are their respective input powers. κ_a is the total decay rate of the optical cavity, which is the sum of the external loss rate $\kappa_{a\rm ex}$ at the input mirror and the intrinsic loss rate $\kappa_{a\rm in}$ inside the cavity. $\delta=\omega_{\rm pr}-\omega_{\rm pu}$ is the frequency detuning of the optical probe field from the pump field, and $\phi_{\rm p}$ is the phase difference between the probe and pump fields. $\varepsilon_d=F\sqrt{1/2\hbar\omega_c m}$ is the amplitude of the external mechanical driving field, where F is the magnitude of the force, and ω_d and ϕ_d are the frequency and the phase of the external mechanical driving field, respectively.

By adopting the quantum Langevin equations (QLEs) for the operators, in which the damping and noise terms are supplemented,[29,62] we obtain

$$\begin{aligned}
\dot{\hat{a}} &= -\left(\mathrm{i}\Delta_a+\frac{\kappa_a}{2}\right)\hat{a}+\mathrm{i}g_{\rm om}\hat{a}(\hat{b}^\dagger+\hat{b})+\varepsilon_{\rm pu}\\
&\quad+\varepsilon_{\rm pr}\mathrm{e}^{-\mathrm{i}\delta t-\mathrm{i}\phi_{\rm p}}+\hat{f}_{\rm in},\\
\dot{\hat{b}} &= -\left(\mathrm{i}\omega_b+\frac{\gamma_b}{2}\right)\hat{b}+\mathrm{i}g_{\rm om}\hat{a}^\dagger\hat{a}+\mathrm{i}J\hat{c}+\hat{\varsigma}_{\rm in},\\
\dot{\hat{c}} &= -\left(\mathrm{i}\omega_c+\frac{\gamma_c}{2}\right)\hat{c}+\mathrm{i}J\hat{b}+\varepsilon_d\mathrm{e}^{-\mathrm{i}\omega_d t-\mathrm{i}\phi_d}+\hat{\xi}_{\rm in}, \qquad (4)
\end{aligned}$$

where γ_b and γ_c are the intrinsic damping rates of mechanical resonators b and c, respectively; $\hat{f}_{\rm in}$ is the optical input noise; and $\hat{\varsigma}_{\rm in}$ and $\hat{\xi}_{\rm in}$ are the quantum Brownian noises acting on the mechanical resonators b and c, respectively.[62] For simplicity, the hat symbols of the operators are omitted in the description below.

Relative to the intensity of the optical pump field, we assume that both the intensities of the optical probe field and the external mechanical driving field satisfy the conditions $\varepsilon_{\rm pr}\ll\varepsilon_{\rm pu}$ and $\varepsilon_d\ll\varepsilon_{\rm pu}$. We then linearize the dynamical equations of the system by assuming $a=a_{\rm s}+\delta a$, $b=b_{\rm s}+\delta b$, and $c=c_{\rm s}+\delta c$, all of which are composed of an average amplitude and a fluctuation term. $a_{\rm s}$, $c_{\rm s}$, and $b_{\rm s}$ are the steady-state values when only the strong optical pump field is applied. Assuming $\varepsilon_{\rm pr}\to 0$, $\varepsilon_d\to 0$ and setting all the time derivatives to zero, we have

$$\begin{aligned}
a_{\rm s} &= \frac{\varepsilon_{\rm pu}}{\mathrm{i}\Delta'_a+\kappa_a/2},\\
b_{\rm s} &= \frac{\mathrm{i}g_{\rm om}|a_s|^2+\mathrm{i}Jc_{\rm s}}{\mathrm{i}\omega_b+\gamma_b/2},\\
c_{\rm s} &= \frac{\mathrm{i}Jb_{\rm s}}{\mathrm{i}\omega_c+\gamma_c/2}, \qquad (5)
\end{aligned}$$

where $\Delta'_a=\Delta_a-g_{\rm om}(b^*_{\rm s}+b_{\rm s})$, Δ'_a is the effective frequency detuning of the optical pump field from the optical cavity, including the frequency shift caused by the mechanical motion. Furthermore, by substituting $a=a_{\rm s}+\delta a$, $b=b_{\rm s}+\delta b$, and $c=c_{\rm s}+\delta c$ into the nonlinear QLEs and dropping the small nonlinear terms, we can obtain the linearized QLEs as follows:

$$\begin{aligned}
\dot{\delta a} &= -\left(\mathrm{i}\Delta'_a+\frac{\kappa_a}{2}\right)\delta a+\mathrm{i}G_{\rm om}(\delta b^\dagger+\delta b)\\
&\quad+\varepsilon_{\rm pr}\mathrm{e}^{-\mathrm{i}\delta t-\mathrm{i}\phi_{\rm p}}+f_{\rm in},\\
\dot{\delta b} &= -\left(\mathrm{i}\omega_b+\frac{\gamma_b}{2}\right)\delta b+\mathrm{i}(G^*_{\rm om}\delta a+G_{\rm om}\delta a^\dagger)+\mathrm{i}J\delta c+\varsigma_{\rm in},\\
\dot{\delta c} &= -\left(\mathrm{i}\omega_c+\frac{\gamma_c}{2}\right)\delta c+\mathrm{i}J\delta b+\varepsilon_d\mathrm{e}^{-\mathrm{i}\omega_d t-\mathrm{i}\phi_d}+\xi_{\rm in}, \qquad (6)
\end{aligned}$$

where $G_{\rm om}=g_{\rm om}a_{\rm s}$ is the total coupling strength between the optical cavity mode a and the mechanical mode b.

We assume that the cavity is driven by the optical pump field at the red sideband $\Delta'_a=\omega_b$ and the system is operated in a resolved sideband regime in which $\omega_b(\omega_c)\gg\kappa_a$. The mechanical resonator also has a high-quality factor for $\omega_b(\omega_c)\gg\gamma_b(\gamma_c)$. For simplicity, we assume that the frequencies of the mechanical resonators b and c are equal, and the frequency of the weak external mechanical driving field is also equal to c, where $\omega_d=\omega_b=\omega_c$. With $\delta=\omega_d$, the fluctuation terms δa, δb, δc and noise terms $f_{\rm in}$, $\varsigma_{\rm in}$, $\xi_{\rm in}$ can be rewritten as

$$\begin{aligned}
\delta a &= \delta a_+\mathrm{e}^{-\mathrm{i}\delta t}+\delta a_-\mathrm{e}^{\mathrm{i}\delta t},\\
\delta b &= \delta b_+\mathrm{e}^{-\mathrm{i}\delta t}+\delta b_-\mathrm{e}^{\mathrm{i}\delta t},\\
\delta c &= \delta c_+\mathrm{e}^{-\mathrm{i}\delta t}+\delta c_-\mathrm{e}^{\mathrm{i}\delta t},\\
f_{\rm in} &= f_{\rm in_+}\mathrm{e}^{-\mathrm{i}\delta t}+f_{\rm in_-}\mathrm{e}^{\mathrm{i}\delta t},\\
\varsigma_{\rm in} &= \varsigma_{\rm in_+}\mathrm{e}^{-\mathrm{i}\delta t}+\varsigma_{\rm in_-}\mathrm{e}^{\mathrm{i}\delta t},\\
\xi_{\rm in} &= \xi_{\rm in_+}\mathrm{e}^{-\mathrm{i}\delta t}+\xi_{\rm in_-}\mathrm{e}^{\mathrm{i}\delta t}, \qquad (7)
\end{aligned}$$

where O_+ and O_- (with $O=a,b,c$) correspond to the components at original frequencies of $\omega_{\rm pr}$ and $2\omega_{\rm pu}-\omega_{\rm pr}$, respectively.[21,63] We substitute Eq. (5) into Eq. (6), and ignore the second-order small terms by equating the coefficients of terms with the same frequency. The component at the frequency $\omega_{\rm pr}$ can be obtained as

$$\begin{aligned}
\dot{\delta a_+} &= \left(\mathrm{i}\lambda_a-\frac{\kappa_a}{2}\right)\delta a_++\mathrm{i}G_{\rm om}\delta b_++\varepsilon_{\rm pr}\mathrm{e}^{-\mathrm{i}\phi_{\rm p}}+f_{\rm in_+},\\
\dot{\delta b_+} &= \left(\mathrm{i}\lambda_b-\frac{\gamma_b}{2}\right)\delta b_++\mathrm{i}G^*_{\rm om}\delta a_++\mathrm{i}J\delta c_++\varsigma_{\rm in_+},\\
\dot{\delta c_+} &= \left(\mathrm{i}\lambda_c-\frac{\gamma_c}{2}\right)\delta c_++\mathrm{i}J\delta b_++\varepsilon_d\mathrm{e}^{-\mathrm{i}\phi_d}+\xi_{\rm in_+}, \qquad (8)
\end{aligned}$$

where $\lambda_a=\delta-\Delta'_a$, $\lambda_b=\delta-\omega_b$, and $\lambda_c=\delta-\omega_c$. They satisfy the relation $\lambda_a=\lambda_b=\lambda_c$.

The noise terms obey the following fluctuations in correlation:

$$\langle\hat{f}_{\rm in}(t)\hat{f}^\dagger_{\rm in}(t')\rangle=[N(\omega_a)+1]\delta(t-t'),$$

$$\begin{aligned}
&\langle \hat{f}_{\rm in}^{\dagger}(t)\hat{f}_{\rm in}(t')\rangle = [N(\omega_a)]\delta(t-t'),\\
&\langle \hat{\varsigma}_{\rm in}(t)\hat{\varsigma}_{\rm in}^{\dagger}(t')\rangle = [N(\omega_b)+1]\delta(t-t'),\\
&\langle \hat{\varsigma}_{\rm in}^{\dagger}(t)\hat{\varsigma}_{\rm in}(t')\rangle = [N(\omega_b)]\delta(t-t'),\\
&\langle \hat{\xi}_{\rm in}(t)\hat{\xi}_{\rm in}^{\dagger}(t')\rangle = [N(\omega_c)+1]\delta(t-t'),\\
&\langle \hat{\xi}_{\rm in}^{\dagger}(t)\hat{\xi}_{\rm in}(t')\rangle = [N(\omega_c)]\delta(t-t'),
\end{aligned} \tag{9}$$

where $N(\omega_a)=[\exp(\hbar\omega_a/k_{\rm B}T)-1]^{-1}$ is the mean number of thermal photons of the optical fields at equilibrium. $N(\omega_b)=[\exp(\hbar\omega_b/k_{\rm B}T)-1]^{-1}$ and $N(\omega_c)=[\exp(\hbar\omega_c/k_{\rm B}T)-1]^{-1}$ are the mean numbers of thermal phonons of the mechanical resonators b and c at equilibrium. To neglect the influence of noise, we assume that our system is operated at sufficiently low temperature and simultaneously satisfies the conditions $\hbar\omega_a/k_{\rm B}T\gg 1$, $\hbar\omega_b/k_{\rm B}T\gg 1$, and $\hbar\omega_c/k_{\rm B}T\gg 1$; correspondingly, $\langle f_{\rm in_+}\rangle=\langle\varsigma_{\rm in_+}\rangle=\langle\xi_{\rm in_+}\rangle=0$.[9,64] Under the mean-field steady-state condition $\langle\delta\dot{a}_+\rangle=\langle\delta\dot{b}_+\rangle=\langle\delta\dot{c}_+\rangle=0$, we can obtain

$$\begin{aligned}
0 &= \left(\mathrm{i}\lambda_a-\frac{\kappa_a}{2}\right)\langle\delta a_+\rangle+\mathrm{i}G_{\rm om}\langle\delta b_+\rangle+\varepsilon_{\rm pr}\,\mathrm{e}^{-\mathrm{i}\phi_{\rm p}},\\
0 &= \left(\mathrm{i}\lambda_b-\frac{\gamma_b}{2}\right)\langle\delta b_+\rangle+\mathrm{i}G_{\rm om}^{*}\langle\delta a_+\rangle+\mathrm{i}J\langle\delta c_+\rangle,\\
0 &= \left(\mathrm{i}\lambda_c-\frac{\gamma_c}{2}\right)\langle\delta c_+\rangle+\mathrm{i}J\langle\delta b_+\rangle+\varepsilon_d\,\mathrm{e}^{-\mathrm{i}\phi_d}.
\end{aligned} \tag{10}$$

The solution of $\langle\delta a_+\rangle$ can be obtained as

$$\begin{aligned}
\langle\delta a_+\rangle = \mathrm{e}^{-\mathrm{i}\phi_{\rm p}}\Bigg[&\frac{-G_{\rm om}J\varepsilon_d\,\mathrm{e}^{-\mathrm{i}\phi}}{(\frac{\kappa_a}{2}-\mathrm{i}\lambda_a)[(\frac{\gamma_b}{2}-\mathrm{i}\lambda_b)(\frac{\gamma_c}{2}-\mathrm{i}\lambda_c)+J^2]+|G_{\rm om}|^2(\frac{\gamma_c}{2}-\mathrm{i}\lambda_c)}\\
&+\frac{[(\frac{\gamma_b}{2}-\mathrm{i}\lambda_b)(\frac{\gamma_c}{2}-\mathrm{i}\lambda_c)+J^2]\varepsilon_{\rm pr}}{(\frac{\kappa_a}{2}-\mathrm{i}\lambda_a)[(\frac{\gamma_b}{2}-\mathrm{i}\lambda_b)(\frac{\gamma_c}{2}-\mathrm{i}\lambda_c)+J^2]+|G_{\rm om}|^2(\frac{\gamma_c}{2}-\mathrm{i}\lambda_c)}\Bigg],
\end{aligned} \tag{11}$$

where $\phi=\phi_d-\phi_{\rm p}$ is the phase difference between the external mechanical driving field and the optical fields. Based on the input–output relation, the output field at probe frequency $\omega_{\rm pr}$ can be expressed as[21,26]

$$\langle\varepsilon_{\rm out}\rangle+\varepsilon_{\rm pu}+\varepsilon_{\rm pr}\,\mathrm{e}^{-\mathrm{i}\phi_{\rm p}}=\kappa_{a\rm ex}\langle\delta a_+\rangle, \tag{12}$$

where $\kappa_{a\rm ex}$ dominates the external loss rate of the cavity, with $\kappa_{a\rm ex}=\sigma\kappa_a$. κ_a is the total decay rate of the optical cavity, which is the sum of the external loss rate $\kappa_{a\rm ex}$ at the input mirror and the intrinsic loss rate $\kappa_{a\rm in}$ inside the cavity. σ is the coupling parameter, which represents the coupling region of the system, and its range is $0\le\sigma\le 1$. Speciallyfic, when $\sigma\ll 1$, the cavity is undercoupling; when $\sigma\simeq 1$, the cavity is overcoupled.[9]

Defining $\varepsilon_{\rm T}=\sigma\kappa_a\langle\delta a_+\rangle/\varepsilon_{\rm pr}$,[11,29] we obtain the quadrature $\varepsilon_{\rm T}$ of the output field at frequency $\omega_{\rm pr}$

$$\varepsilon_{\rm T} = \sigma\kappa_a\left[\frac{-|G_{\rm om}|J\eta\,\mathrm{e}^{-\mathrm{i}\phi}}{(\frac{\kappa_a}{2}-\mathrm{i}\lambda_a)[(\frac{\gamma_b}{2}-\mathrm{i}\lambda_b)(\frac{\gamma_c}{2}-\mathrm{i}\lambda_c)+J^2]+|G_{\rm om}|^2(\frac{\gamma_c}{2}-\mathrm{i}\lambda_c)}+\frac{(\frac{\gamma_b}{2}-\mathrm{i}\lambda_b)(\frac{\gamma_c}{2}-\mathrm{i}\lambda_c)+J^2}{(\frac{\kappa_a}{2}-\mathrm{i}\lambda_a)[(\frac{\gamma_b}{2}-\mathrm{i}\lambda_b)(\frac{\gamma_c}{2}-\mathrm{i}\lambda_c)+J^2]+|G_{\rm om}|^2(\frac{\gamma_c}{2}-\mathrm{i}\lambda_c)}\right], \tag{13}$$

where $\eta=\varepsilon_d/\varepsilon_{\rm pr}$ is the ratio of the amplitude of the external mechanical driving field to that of the optical probe field. The transmission coefficient and the power transmission coefficient are further defined as $\mathcal{T}=-1+\varepsilon_{\rm T}$ and $T=|\mathcal{T}|^2$, respectively.[29] $\mathrm{Re}[\varepsilon_{\rm T}]$ and $\mathrm{Im}[\varepsilon_{\rm T}]$ are the real part and imaginary part of $\varepsilon_{\rm T}$, they describe the absorptive and dispersive behaviors of the probe field, respectively.[26,29]

If we assume that no external mechanical driving field is applied to the additional mechanical resonator c, defining $\lambda=\lambda_a=\lambda_b$, then after the simplification, the term $\varepsilon_{\rm T}$ becomes

$$\varepsilon_{\rm T}=\frac{\sigma\kappa_a}{\frac{\kappa_a}{2}-\mathrm{i}\lambda+\frac{A_+}{\lambda_+-\mathrm{i}\lambda}+\frac{A_-}{\lambda_--\mathrm{i}\lambda}}, \tag{14}$$

where

$$\lambda_\pm=\frac{\frac{\gamma_b}{2}+\frac{\gamma_c}{2}\pm\mathrm{i}\sqrt{4J^2-(\frac{\gamma_b}{2}-\frac{\gamma_c}{2})^2}}{2},$$

$$A_\pm=\pm\frac{\lambda_\pm-\frac{\gamma_c}{2}}{\lambda_+-\lambda_-}|G_{\rm om}|^2. \tag{15}$$

This expression has the standard form for the double OMIT, which is similar to the double EIT.[65] If we eliminate the coupling interaction between mechanical resonators b and c, $\varepsilon_{\rm T}$ becomes

$$\varepsilon_{\rm T}=\frac{\sigma\kappa_a}{\frac{\kappa_a}{2}-\mathrm{i}\lambda_a+\frac{|G_{\rm om}|^2}{\gamma_b/2-\mathrm{i}\lambda_b}}, \tag{16}$$

and has the standard form of the single-OMIT window, which is similar to the standard EIT.[30]

3. Physical mechanism of the system

We now discuss the feasibility of the tunable double OMIT for the hybrid optomechanical cavity system. To en-

sure that the double-OMIT can be generated, the total optomechanical coupling strength should meet the condition $G_{\rm om} > \sqrt{\kappa_a \gamma_m}/2$, in which a typical single-OMIT phenomenon can be obtained when only the pump and the probe fields are applied.[29] Moreover, in our system, the strength of coupling between the two mechanical resonators meets the condition $J > \gamma_b/2$, otherwise, the new dressed energy-levels will be covered by the line-width of the mechanical resonators. For the sake of simplicity, we assume that the system is over-coupled; i.e., the coupling parameter $\sigma = 1$.

Correspondingly, we choose the power of the pump field $P_{\rm pu} = 0.08$ mW, $P_{\rm pr} = P_{\rm pu}/10 = 0.008$ mW. The optical cavity is driven by the optical pump field on the red sideband, where $\Delta_a' = \omega_m$. The parameters of the system we chose are shown below, and are all based on the realistic system.[66] The frequency and decay rate of the optical cavity are $\omega_a/2\pi =$ 194 THz and $\kappa_a/2\pi = 215$ kHz. For simplicity, we assume that the frequencies of the mechanical resonators b and c are equal, which are set at $\omega_b/2\pi = \omega_c/2\pi = \omega_m/2\pi = 947$ kHz. The two mechanical resonators have high-quality factors for $\gamma_b/2\pi = \gamma_c/2\pi = 140$ Hz, which strictly meet the condition of the sideband-resolved regime $\omega_b > \kappa_a$. The qualities of the two mechanical resonators are equal, $m_b = m_c = 145$ ng. The strength of the single-photon optomechanical coupling is $g_{\rm om}/2\pi = 2.7$ Hz. Furthermore, we assume that the strength of coupling between the mechanical resonators b and c is $J/2\pi = 4.68$ kHz.[16]

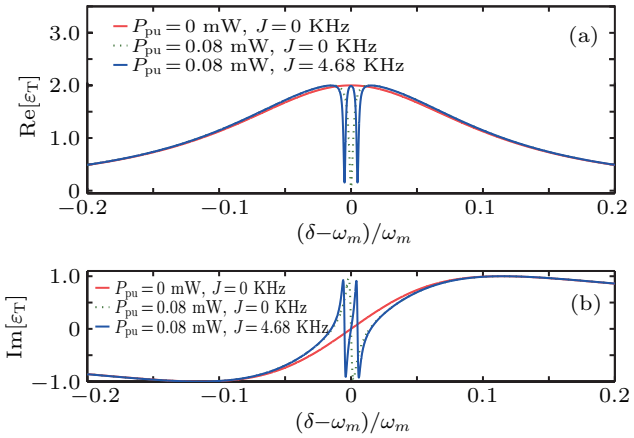


Fig. 2. (a) The real part Re[$\varepsilon_{\rm T}$] and (b) imaginary part Im[$\varepsilon_{\rm T}$] as a function of $(\delta - \omega_m)/\omega_m$ for the cavity system under the condition of no external mechanical driving field applied, with parameters $P_{\rm pr} = 0.008$ mW, $\sigma = 1$, $g_{\rm om}/2\pi = 2.7$ Hz, $\kappa_a/2\pi = 215$ kHz, $\omega_a/2\pi = 194$ THz, $\omega_b/2\pi = \omega_c/2\pi = \omega_m/2\pi = 947$ kHz, $\gamma_b/2\pi = \gamma_c/2\pi = 140$ Hz, $m_b = m_c = 145$ ng, and $\Delta_a' = \omega_b = \omega_c$.

We first consider the situation that there is no external driving applied to the mechanical resonator c, as shown in Figs. 2(a) and 2(b). The real part Re[$\varepsilon_{\rm T}$] and the imaginary part Im[$\varepsilon_{\rm T}$] of the optical probe field as a function of $(\delta - \omega_m)/\omega_m$ are plotted, which exhibit the absorptive and the dispersive behaviors of the probe field, respectively. When the pump field is applied to the optical system, in the transmission spectrum, a double-transparency window can be obtained and the positions of two minima are determined by the imaginary parts of $\lambda_\pm$, as shown by the solid curve. The distance between the minima is $2J$, which is closely related to the strength of coupling between the mechanical resonators b and c. If there is no coupling interaction between the mechanical resonators b and c, as shown by the dashed curve, a single-transparency window in the transmission spectrum curve can be obtained. In this situation, the minima point is determined by the frequency point $\delta = \omega_m$, and the relevant mechanisms have been studied extensively.[26] Moreover, if no pump field is applied to the optical cavity a, then no transparency window appears, as shown by the dotted curve.

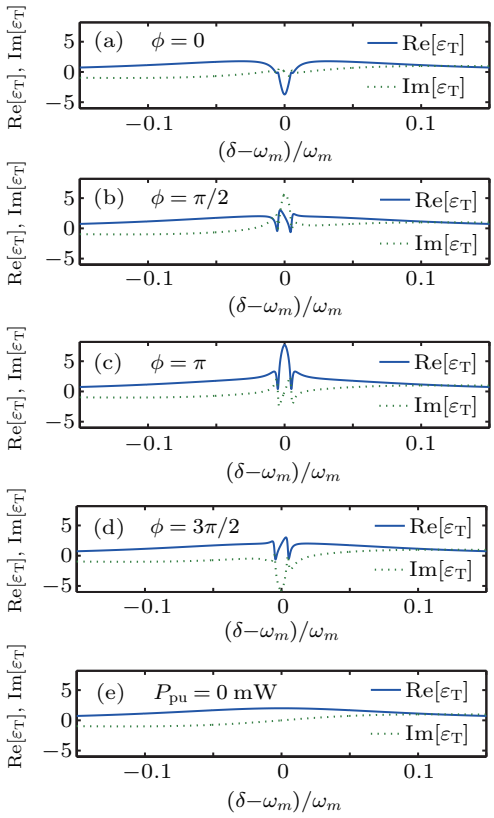


Fig. 3. The real part Re[$\varepsilon_{\rm T}$] (solid line) and imaginary part Im[$\varepsilon_{\rm T}$] (dashed line) as a function of $(\delta - \omega_m)/\omega_m$ for different phase factors: (a) $\eta = 1$, $\phi = 0$; (b) $\eta = 1$, $\phi = \pi/2$; (c) $\eta = 1$, $\phi = \pi$; (d)$\eta = 1$, $\phi = 3\pi/2$; (e) $\eta = 0$, $P_{\rm pu} = 0$. The other parameters are identical to those in Fig. 2.

We now consider the situation where a weak external coherently mechanical driving field is applied to the system. For simplicity, we assume that the frequency of the mechanical driving field is equal to c, where $\omega_d = \omega_c$, then we have $\omega_d = \omega_m = \omega_b = \omega_c$. We also assume that the amplitude-ratio η meets the condition $\eta = \varepsilon_d/\varepsilon_{\rm pr} = 1$. In Figs. 3(a)–3(d), we plot the real part Re[$\varepsilon_{\rm T}$] and the imaginary part Im[$\varepsilon_{\rm T}$] of the optical probe field as a function of $(\delta - \omega_m)/\omega_m$ for different phase differences ϕ. It is shown that when $\phi = 0$ and $\phi = \pi$, thee absorptive and the dispersive behavior curves are symmetric and antisymmetric, respectively. The difference between the

situations $\phi = 0$ and $\phi = \pi$ is that when $\phi = 0$, the destructive interference between the two terms in Eq. (12) suppresses the absorptive behavior at frequency $\delta = \omega_m$; when $\phi = \pi$, the constructive interference between the terms in Eq. (12) amplifies the absorptive behavior at frequency $\delta = \omega_m$. It is shown that when $\phi = \pi/2$ and $\phi = 3\pi/2$, the absorptive and the dispersive behavior curves are both anomalous, and the maxima of the absorptive and the dispersive behavior curves appear in the red- or blue-detuned regions, respectively. In particular, comparing the situations of $\phi = \pi/2$ and $\phi = 3\pi/2$, it is evident that the absorptive behavior curves are mirror symmetric between them. For comparison, in the absence of the optical pump field, the real part $\mathrm{Re}[\varepsilon_T]$ and imaginary part $\mathrm{Im}[\varepsilon_T]$ of the optical probe field are also shown in Fig. 3(e).

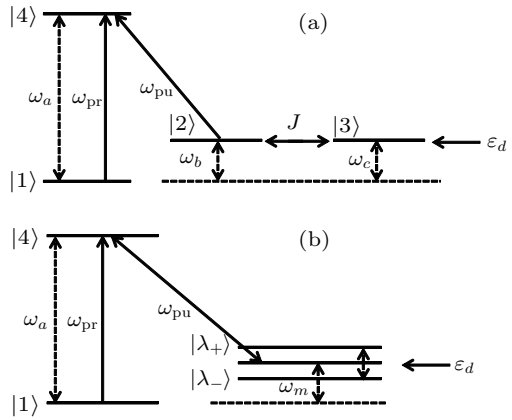


Fig. 4. (a) Energy-level structure of the hybrid optomechanical system, where the states of the levels are $|i\rangle$ $(i = 1,2,3,4)$. The amplitude of the external mechanical driving field is ε_d. The energy differences between $|1\rangle$ and $|4\rangle$, $|1\rangle$ and $|2\rangle$, and $|1\rangle$ and $|3\rangle$ are the frequencies of cavity a, mechanical resonator b, and mechanical resonator c, which are ω_a, ω_b, and ω_c, respectively. ω_{pr} is equal to ω_a, and the detuning events between them are $\omega_{pr} - \omega_{pu} = \omega_b = \omega_c$. (b) Energy-level structure of the hybrid optomechanical system in the dressed-state picture, with the relation $\omega_b = \omega_c = \omega_m$. $|\lambda_\pm\rangle$ are the new dressed levels generated by the coupling effect between the mechanical resonators, with an energy difference of $2J$.

The standard double-transparency window shown in Fig. 2(a) originates from the quantum interference effect between different energy level pathways. In the hybrid optomechanical system, a four-level energy configuration is formed by the energy levels of the optical cavity and the mechanical resonators. Under the coupling effect between the mechanical resonators b and c, the original energy level of the mechanical resonator ω_m level is split into two new dressed levels. With $\Delta_a' = \omega_m = \omega_b = \omega_c$, the two new dressed levels are $\lambda_\pm$, and the disparity between them is $2J$, as shown in Fig. 4(b). Under the effects of optical radiation pressure, quantum interference between different energy level pathways occurs, the third-order nonlinear absorption is enhanced by a constructive quantum interference, and the linear absorption is inhibited by a destructive quantum interference. Consequently, the double-OMIT window appears, and the relevant mechanisms have been studied extensively.[67,68]

Comparing Fig. 3 with Fig. 2, it is shown that when a weak external mechanical driving field is applied to the mechanical resonator c, the absorptive and dispersive behavior curves at frequency $\delta = \omega_m$ are modulated prominently by the phase of the external mechanical driving field. This phenomenon is consistent with Eq. (11), which is composed of two different terms, the first term is dominated by the external mechanical driving field and the second term is dominated by the optical fields. When the optical pump and the optical probe fields are applied to the system, in the absence of the external mechanical driving field, the value of the first term is zero and a standard double-OMIT can be generated. When the external mechanical driving field is also applied to the system, the first term turns into a nonzero value, then the standard double-OMIT is modulated, as shown in Figs. 3(a)–3(d). Typically, under the situation $\phi = 0$ or $\phi = \pi$, equation (11) becomes

$$\varepsilon_T = \sigma\kappa_a\left[\frac{\pm|G_{om}|J\eta + [(\frac{\gamma_b}{2} - i\lambda_b)(\frac{\gamma_c}{2} - i\lambda_c) + J^2]}{(\frac{\kappa_a}{2} - i\lambda_a)[(\frac{\gamma_b}{2} - i\lambda_b)(\frac{\gamma_c}{2} - i\lambda_c) + J^2] + |G_{om}|^2(\frac{\gamma_c}{2} - i\lambda_c)}\right], \tag{17}$$

where "−" and "+" correspond to the phase-difference $\phi = 0$ and $\phi = \pi$, respectively. When $\phi = 0$, the destructive interference between the external mechanical driving field and the optical fields can be generated, as shown in Fig. 3(a). When $\phi = \pi$, the constructive interference between the external mechanical driving field and the optical fields can be generated, as shown in Fig. 3(c).

Physically, this phenomenon arises because the energy levels of the system are modulated by the external mechanical driving field. As shown in Fig. 4(b), under the coupling between the mechanical resonators b and c, the energy level of the original mechanical resonator ω_m turns into an empty-level state. When the external mechanical driving field is applied to the mechanical resonator c, with the condition that the frequency of the mechanical driving field is equal to the frequency of the mechanical resonator, the number of phonons with frequency ω_m is increased, then the empty mechanical resonator level is replenished into an occupied state by the mechanical driving field. Meanwhile, when the optical pump field is applied on the red-detuned sideband of the cavity, the number of phonons with frequency ω_m is decrease by the sideband-cooling effect of the pump field. As the population of phonons with frequency ω_m can be controlled by both the mechanical field and the optical fields, under the destructive or constructive quantum interference between the mechanical-phonons and optical-photons, the absorptive and dispersive be-

havior curves near frequency $\delta = \omega_m$ are modulated, as shown in Eq. (11). Consequently, the optical probe field is absorbed excessively or amplified remarkably, which is consistent with Eq. (11). A similar mechanism has also been studied in the single-OMIT systems.[29]

4. Tunable double OMIT controlled by the phase and amplitude of the external mechanical driving field

To explore the effect of the external mechanical driving field, we plot the real part $\mathrm{Re}[\varepsilon_T]$ as a function of $(\delta-\omega_m)/\omega_m$ and η, where $\eta = \varepsilon_d/\varepsilon_{pr}$. We consider the situation in which the phase difference between the mechanical driving field and the optical fields meets the condition $\phi = 0$, as shown in Fig. 5. In the absence of the mechanical driving field, when $\eta = 0$, under interference between the optical pump field and the optical probe field, a standard double OMIT window appears. With the enhancement of the mechanical driving intensity, the absorption rate at frequency $\delta = \omega_m$ gradually decreases from positive to negative, where the narrow probe curve at frequency $\delta = \omega_m$ is modulated from full opacity to remarkable amplification. More importantly, when $\eta = 0.5$, the transmission curve is converted into a standard single-OMIT window, where the probe field at frequency $\delta = \omega_m$ is transmitted perfectly. This phenomenon arises from the destructive quantum interference between the optical fields and the mechanical driving field, which is consistent with Eq. (11).

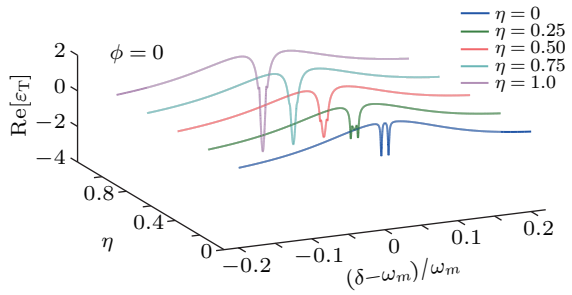


Fig. 5. The real part $\mathrm{Re}[\varepsilon_T]$ as a function of $(\delta-\omega_m)/\omega_m$ and η under the condition $\phi = 0$. The values of η are 1, 0.25, 0.5, 0.75, 1.0; the forces corresponding to them are $F = 9\times10^{-9}$ N, 18×10^{-9} N, 27×10^{-9} N, 36×10^{-9} N, 45×10^{-9} N, respectively. The other parameters are the same as those in Fig. 2.

Furthermore, we discuss the situation that the phase difference between the mechanical driving field and the optical fields meets the condition $\phi = \pi$. As shown in Fig. 6, which shows the real part $\mathrm{Re}[\varepsilon_T]$ as a function of $(\delta-\omega_m)/\omega_m$ and η, in the absence of the mechanical driving field, the transmission spectrum has a standard double-OMIT window. With the enhancement of the mechanical driving intensity, the absorption rate at frequency $\delta = \omega_m$ is increased, and the narrow probe curve at frequency $\delta = \omega_m$ is modulated from full opacity to excessive opacity. Consequently, the intensity of the probe field in the cavity is enhanced. This phenomenon is opposite to the situation shown in Fig. 5, which originates from the constructive quantum interference between the optical fields and the mechanical driving field, which is also consistent with Eq. (11).

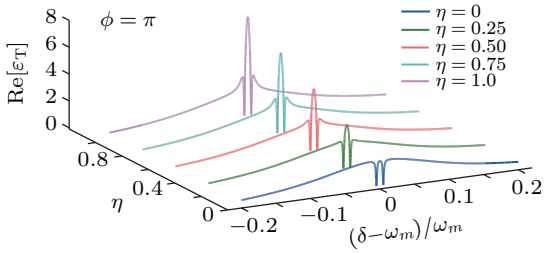


Fig. 6. The real part $\mathrm{Re}[\varepsilon_T]$ as a function of $(\delta-\omega_m)/\omega_m$ and η under the condition $\phi = \pi$. The values of η are 1, 0.25, 0.5, 0.75, 1.0; the forces corresponding to them are $F = 9\times10^{-9}$ N, 18×10^{-9} N, 27×10^{-9} N, 36×10^{-9} N, 45×10^{-9} N, respectively. The other parameters are the same as those in Fig. 2.

In the case of $\phi = 0$ or $\phi = \pi$, the real part $\mathrm{Re}[\varepsilon_T]$ of the optical probe field at the frequency $\delta = \omega_m$ can be obtained. As $\lambda_a = \lambda_b = \lambda_c = 0$, $\mathrm{Re}[\varepsilon_T]$ can be obtained as

$$\mathrm{Re}[\varepsilon_T] = \sigma\kappa_a\left[\frac{\pm|G_{om}|J\eta + \frac{\gamma_b\gamma_c}{4} + J^2}{\frac{\kappa_a}{2}(\frac{\gamma_b\gamma_c}{4} + J^2) + |G_{om}|^2\frac{\gamma_c}{2}}\right]. \tag{18}$$

Specifically, when $\phi = 0$, if we set $\mathrm{Re}[\varepsilon_T] = 0$, we can obtain $\eta = \frac{\gamma_b\gamma_b + 4J^2}{4G_{om}J}$, which corresponds to the situation that the absorption at the frequency $\delta = \omega_m$ is zero. As shown in Fig. 5, when $\eta \simeq 0.5$, the transmission curve converts to a standard single-OMIT window, and the probe field at the frequency $\delta = \omega_m$ is transmitted perfectly.

In addition, as shown in Fig. 2(a), in the double OMIT, the bandwidth of the probe field at frequency $\delta = \omega_m$ is determined by the imaginary parts of $\lambda_\pm$, where $\Gamma_p = \mathrm{i}(\lambda_+ - \lambda_-)/2 \simeq J$. In case of the single OMIT, the bandwidth Γ_p of the probe field at frequency $\delta = \omega_m$ is determined by the delay rates of cavity a and mechanical resonator b, the total optomechanical coupling strength is G_{om}, where $\Gamma_p = \gamma_b + 4{G_{om}}^2/\kappa$.[9] In the absence of the pump field, the bandwidth of the probe field is equal to the delay rate of cavity a, where $\Gamma_p = \kappa_a$.[9] Consequently, the double-OMIT can be applied to generated the high-resolution spectroscopy, in the case that the coupling strength meets the conditions $J \le \gamma_b + 4{G_{om}}^2/\kappa$ and $J \le \kappa_a$.

Based on Figs. 5 and 6, when the phase of the external mechanical driving field meets either condition $\phi = 0$ or $\phi = \pi$, the rate of absorption at frequency $\delta = \omega_m$ is proportional to the intensity of the external driving field. Consequently, the curve of the narrow probe can be modulated from excessive opacity to remarkable amplification. This phenomenon can be applied to many fields. For example, as the transmission spectrum can be changed from the double windows to the single window, our system can be applied to implement double-channel quantum information processing and

optical switching. Similar phenomena have been studied in natural atomic systems.[69,70] Moreover, the line width of the curve of narrow transmission at frequency $\delta = \omega_m$ is approximately equal to J, which is small enough relative to the line width of the optical cavity. Thus, our system can be applied to tunable high-resolution spectroscopy, which is similar to the sub-Doppler spectral resolution observed in natural atomic systems.[71]

5. Tunable double-OMIT controlled by other parameters of the system

We further explore the tunable double-OMIT controlled by other parameters of the system, under the assumption that $G_{\rm om} > \sqrt{\kappa_a \gamma_m}/2$ and $J > \gamma_b/2$. In Fig. 7, we plot the real part $\mathrm{Re}[\varepsilon_{\rm T}]$ as a function of $(\delta - \omega_m)/\omega_m$ and $P_{\rm pu}$ with different powers of the mechanical driving fields. It is shown that when the system is driven by both the optical fields and the mechanical field, with the increasing power of the optical pump field, both the absorptive (when $\phi = \pi$) and gain (when $\phi = 0$) behavior curves of the optical probe field are increased firstly and then decreased at the frequency $\delta = \omega_m$. Based on Eq. (16), by setting $\mathrm{dRe}[\varepsilon_{\rm T}]/\mathrm{d}|G_{\rm om}| = 0$, $\mathrm{d}^2\mathrm{Re}[\varepsilon_{\rm T}]/\mathrm{d}|G_{\rm om}|^2 < 0$ (when $\phi = \pi$), or $\mathrm{d}^2\mathrm{Re}[\varepsilon_{\rm T}]/\mathrm{d}|G_{\rm om}|^2 > 0$ (when $\phi = 0$), we can obtain the maximum point $G_{\rm max}$ (when $\phi = \pi$) and the minimum point $G_{\rm min}$ (when $\phi = 0$) of the absorptive behavior curves, which are $G_{\rm max} \simeq G_{\rm min} \simeq \sqrt{\frac{4J^2\kappa_a + \gamma_b \kappa_a{}^2}{4\gamma_c}}$. Moreover, when we assume $\sigma = 1$, based on the power transmission coefficient $T = |-1 + \varepsilon_{\rm T}|^2$, the transmission coefficient at the frequency $\delta = \omega_m$ can be expressed as

$$T = \left(\frac{\pm |G_{\rm om}| J\eta + \frac{\kappa_a \gamma_b \gamma_c}{8} + \frac{\kappa_a J^2}{2}}{\frac{\kappa_a \gamma_b \gamma_c}{8} + \frac{\kappa_a J^2}{2} + \frac{|G_{\rm om}|^2 \gamma_c}{2}} \right)^2. \tag{19}$$

When $\phi = 0$ and $G_{\rm min} = \sqrt{\frac{4J^2\kappa_a + \gamma_b \kappa_a{}^2}{4\gamma_c}}$, the maximum amplitude of the probe field can be obtained as $T_{\rm max} = \kappa_a \eta^2/\gamma_c$. Moreover, based on the linear-regime analysis, as we have assumed that $\langle \delta_{\hat{c}} \rangle / c_{\rm s} \ll 1$, we estimate that the maximum amplitude $T_{\rm max}$ should meet the condition $\sqrt{T_{\rm max}}|\varepsilon_{\rm pr}|/|\varepsilon_{\rm pu}| \ll 1$. Relative to theoptomechanically induced amplification (OMIA), our system can realize the switch between the excessive absorption and remarkable amplification without changing the frequency of the pump field.

Physically, in Fig. 7, with the driving of the external mechanical field, the number of phonons with frequency ω_m is increased by the excitation of the mechanical field. This progress can enhance the photon–phonon interaction strength between the external mechanical field and the optical fields. On the other hand, when the optical pump field is applied on the red-detuned sideband, the mechanical resonator b is cooled by the pump field, then the number of phonons with frequency ω_m is decreased. This progress can decrease the photon-sphonon interaction strength between the external mechanical field and the optical fields. Consequently, under the combined effects of the mechanical field and the optical fields, a maximum amplitude exists for the probe field, as shown in Fig. 7.

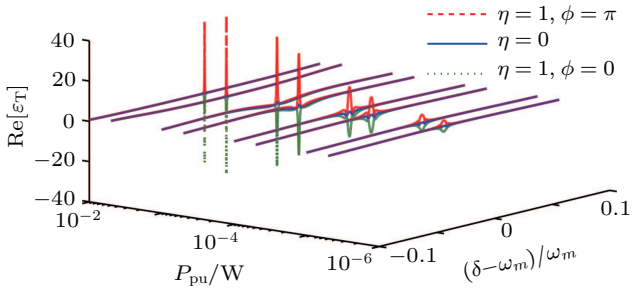


Fig. 7. The real part $\mathrm{Re}[\varepsilon_{\rm T}]$ as a function of $(\delta - \omega_m)/\omega_m$ and $P_{\rm pu}$ ($P_{\rm pu}$ was 0.04×10^{-3} mW) with different powers of optical pump fields under different situations: $\eta = 1$, $\phi = \pi$ (red dashed curve); $\eta = 0$ (blue solid curve); $\eta = 1$, $\phi = 0$ (green dotted curve). The powers of the optical pump fields are $P_{\rm pu} = 0.004$ mW, 0.008 mW, 0.04 mW, 0.08 mW, 0.4 mW, 0.8 mW, 4 mW, 8 mW, respectively. The other parameters are the same as those in Fig. 2.

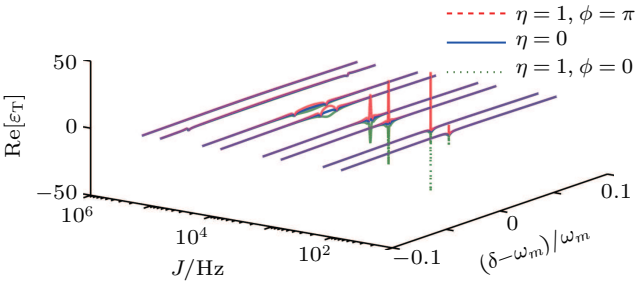


Fig. 8. The real part $\mathrm{Re}[\varepsilon_{\rm T}]$ as a function of $(\delta - \omega_m)/\omega_m$ and J (J was $2\pi \times 8$ kHz) with different mechanical driving fields under different situations: $\eta = 1$, $\phi = \pi$ (red dashed curve); $\eta = 0$(blue solid curve); $\eta = 1$, $\phi = 0$ (green dotted curve). The coupling strength is $J/2\pi = 0.07$ kHz, 0.14 kHz, 0.7 kHz, 1.4 kHz, 7 kHz, 14 kHz, 70 kHz, 140 kHz, respectively. The other parameters are the same as those in Fig. 2.

Figure 8 presents the real part $\mathrm{Re}[\varepsilon_{\rm T}]$ as a function of $(\delta - \omega_m)/\omega_m$ and J with different powers of the mechanical driving fields. It shows that when both the optical fields and the weak mechanical field are applied to the system, with the increasing strength of the coupling J, both the rates of absorption (when $\phi = \pi$) and gain (when $\phi = 0$) are also increased firstly and then decreased. Meanwhile, the line-width of the optical probe field at the frequency $\delta = \omega_m$ is broadened constantly. Based on Eq. (16), by setting $\mathrm{dRe}[\varepsilon_{\rm T}]/\mathrm{d}J = 0$, $\mathrm{d}^2\mathrm{Re}[\varepsilon_{\rm T}]/\mathrm{d}J^2 < 0$ (when $\phi = \pi$), or $\mathrm{d}^2\mathrm{Re}[\varepsilon_{\rm T}]/\mathrm{d}J|^2 > 0$ (when $\phi = 0$), we can obtain the maximum point $J_{\rm max}$ (when $\phi = \pi$) and the minimum point $J_{\rm min}$ (when $\phi = 0$) of the absorptive behavior curves, which are $J_{\rm max} \simeq J_{\rm min} \simeq \sqrt{\frac{\gamma_b \kappa_a{}^2 + 4\gamma_c |G_{\rm om}|^2}{4\kappa_a}}$. Physically, in Fig. 8, with the enhancement of the coupling strength, the number of photons exchanged between the two mechanical resonators is increased. This progress can enhance the photon–phonon interaction strength between the external mechanical field and the optical fields. On the other hand,

with the enhancement of the coupling strength, the line-width of the optical probe field is broadened constantly, the number of phonons excited by the external mechanical field exactly with the frequency ω_m is reduced. This progress can decrease the photon–phonon interaction strength between the external mechanical field and the optical fields. Consequently, under the combined effects of these two progresses, a maximum amplitude also exists for the probe field in this situation.

In general, we consider the situation in which the frequencies of two mechanical resonators b and c are slightly different. In Fig. 9, the real part $\mathrm{Re}[\varepsilon_{\mathrm{T}}]$ as a function of $(\delta-\omega_m)/\omega_m$ for the two mechanical resonators with different frequencies is illustrated. When the system is pumped only by the optical field, relative to the case of $\omega_c=\omega_b$, the absorptive behavior curves move leftward (rightward) in case of $\omega_c<\omega_b$ ($\omega_c>\omega_b$). When the mechanical field is also applied to the system, the rates of absorption (when $\phi=\pi$) and gain (when $\phi=0$) of the optical probe field are both increased. Relative to the case of $\omega_c=\omega_b$, the frequencies of the absorption and gain peaks move leftward (rightward) when $\omega_c<\omega_b$ ($\omega_c>\omega_b$). In addition, relative to the case of $\omega_c=\omega_b$, the absorptive behavior curves (when $\phi=\pi$) and the gain curves (when $\phi=0$) are both asymmetry, the rates of absorption peaks and gain peaks of the optical probe field are also larger than those in the case of $\omega_c=\omega_b$. This phenomenon shows that in the situation of two slightly different mechanical resonators, the phase-dependent double OMIT driven by the mechanical field can still be generated.

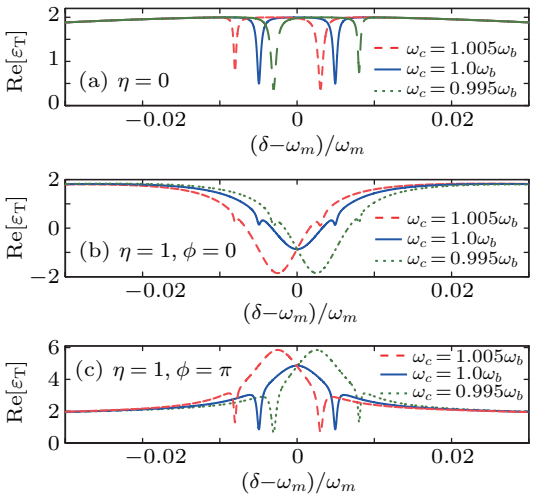


Fig. 9. The real part $\mathrm{Re}[\varepsilon_{\mathrm{T}}]$ as a function of $(\delta-\omega_m)/\omega_m$ for the mechanical resonators with different frequencies. The mechanical driving fields are (a) $\eta=0$; (b) $\eta=1$, $\phi=0$; and (c) $\eta=1$, $\phi=\pi$. The frequencies of the two mechanical resonators are $\omega_c=1.005\omega_b$ (red dashed curves); $\omega_c=1.0\omega_b$ (blue solid curves); $\omega_c=0.995\omega_b$ (green dotted curves). The other parameters are the same as those in Fig. 2.

6. Conclusion

The hybrid optomechanical cavity system proposed here provides a feasible way to control the double OMIT by a weak external mechanical driving field. In this system, the empty state dressed by the coupling effect between the mechanical resonators can be replenished into an occupied state by an external coherently mechanical driving field. Under interference between the optical pumped field and the external mechanical driving field, the absorption and dispersion of the probe field are modulated. It is shown that both the intensity and the phase of the external coherently mechanical driving field can control the propagation of the probe field, including changing the transmission spectrum from double window to single window. Our system can be used to implement tunable, high-resolution spectroscopy and optical switching. More importantly, our system can be extended to other hybrid, solid-state systems to explore new quantum phenomena.

References

[1] Lejman M, Vaudel G, Infante I C, Chaban I, Pezeril T, Edely M, Nataf G F, Guennou M, Kreisel J, Gusev V E, Dkhil B and Ruello P 2016 *Nat. Commun.* **7** 12345
[2] Andrews R W, Peterson R W, Purdy T P, Cicak K, Simmonds R W, Regal C A and Lehnert K W 2014 *Nat. Phys.* **10** 321
[3] Verhagen E, Delaiaeglise S, Weis S, Schliesser A and Kippenberg T J 2012 *Nature* **482** 63
[4] Bochmann J, Vainsencher A, Awschalom D D and Cleland A N 2013 *Nat. Phys.* **9** 712
[5] Balram K C, Davanco M I, Song J D and Srinivasan K 2016 *Nat. Photon.* **10** 346
[6] Jing C, Cui Y S, Liu H X, Li X W and Chen G B 2018 *Chin. Phys. B* **27** 24204
[7] Liu Y L, Wang C, Zhang J and Liu Y X 2018 *Chin. Phys. B* **27** 24204
[8] Wu S C, Qin L G, Jing J, Yang G H and Wang Z Y 2016 *Chin. Phys. B* **25** 54203
[9] Aspelmeyer M, Kippenberg T J and Marquardt F 2014 *Rev. Mod. Phys.* **86** 1391
[10] Fan L, Fong K Y, Poot M and Tang H X 2015 *Nat. Commun.* **6** 5850
[11] Weis S, Riviere R, Deleglise S, Gavartin E, Arcizet O, Schliesser A and Kippenberg T J 2010 *Science* **330** 1520
[12] Xiao Y, Yu Y F and Zhang Z M 2014 *Opt. Express* **22** 17979
[13] Jinag C, Cui Y S, Zhai Z Y, Yu H L, Li X W and Chen G B 2018 *Opt. Express* **26** 28834
[14] Yang Q, Hou B P and Lai D G 2017 *Opt. Express* **25** 9697
[15] Xiong H and Wu Y 2018 *Appl. Phys. Rev.* **5** 031305
[16] Lin Q, Rosenberg J, Chang D, Camacho R, Eichenfield M, Vahala K J and Painter O 2010 *Nat. Photon.* **4** 236
[17] Ma P C, Zhang J Q, Xiao Y, Feng M and Zhang Z M 2014 *Phys. Rev. A* **90** 043825
[18] Regal C, Teufel J and Lehnert K 2008 *Nat. Phys.* **4** 555
[19] Sanchez D G, Daiaeleglise S, Thomas J L, Atkinson P, Lagoin C and Perrin B 2016 *Phys. Rev. A* **94** 033813
[20] Balram K C, Davanco M I, Ilic B R, Kyhm J H, Song J D and Srinivasan K 2017 *Phys. Rev. Appl.* **7** 024008
[21] Zhang J Q, Li Y, Feng M and Xu Y 2012 *Phys. Rev. A* **86** 053806
[22] Gaidarzhy A, Zolfagharkhani G, Badzey R L and Mohanty P 2005 *Phys. Rev. Lett.* **94** 030402
[23] Xue F, Wang Y D, Sun C P, Okamoto H, Yamaguchi H and Semba K 2007 *New J. Phys.* **9** 35
[24] Wang Q, Zhang J Q, Ma P C, Yao C M and Feng M 2015 *Phys. Rev. A* **91** 063827
[25] Zhang H, Saif F, Jiao Y and Jing H 2018 *Opt. Express* **26** 25199
[26] Agarwal G S and Huang S 2010 *Phys. Rev. A* **81** 041803
[27] Xiang Z L, Ashhab S, You J Q and Nori F 2013 *Rev. Mod. Phys.* **85** 623
[28] Safavi-Naeini A H, Alegre T M, Chan J, Eichenfield M, Winger M, Lin Q, Hill J T, Chang D E and Painter O 2011 *Nat. (London)* **472** 69
[29] Jia W Z, Wei L F, Li Y and Liu Y X 2015 *Phys. Rev. A* **91** 043843
[30] Harris S E 1997 *Phys. Today* **50** 36
[31] Boller K J, Imamoglu A and Harris S E 1991 *Phys. Rev. Lett.* **66** 2593
[32] Xu J and Huang G 2013 *Opt. Express* **25** 33575

[33] Cheng H, Wang H M, Zhang S S, Xin P P, Luo J and Liu H P 2017 *Opt. Express* **472** 69
[34] Bienert M and Blostein P B 2015 *Phys. Rev. A* **91** 023818
[35] Zhang S, Zhang J Q, Zhang J, Wu C W, Wu W and Chen P X 2014 *Opt. Express* **22** 28118
[36] Akram M J, Khan M M and Saif F 2015 *Phys. Rev. A* **92** 023846
[37] Jiang C, Liu H, Cui Y, Li X, Chen G and Chen B 2013 *Opt. Express* **21** 12165
[38] Stannigel K, Rabl P, Sorensen A S, Lukin M D and Zoller P 2011 *Phys. Rev. A* **84** 042341
[39] Mcgeev S A, Meiser D, Regal C A, Lehnert K W and Holland M J 2013 *Phys. Rev. A* **87** 053818
[40] Wu Q, Zhang J Q, Wu J H, Feng M and Zhang Z M 2015 *Opt. Express* **23** 18534
[41] Li L C, Shi R, Xu J and Hu X M 2015 *Chin. Phys. B* **24** 054205
[42] Wang H, Gu X, Liu Y X, Miranowicz A and Nori F 2014 *Phys. Rev. A* **90** 023817
[43] Qu K and Agarwal G S 2013 *Phys. Rev. A* **87** 031802
[44] Gu W G and Yi Z 2014 *Opt. Commun.* **333** 261
[45] Wu S C, Qin L G, Jing J, Yan T M, Lu J and Wang Z Y 2018 *Phys. Rev. A* **98** 013807
[46] Harris S E and Yamamoto Y 1998 *Phys. Rev. Lett.* **81** 3611
[47] Yan M, Rickey E G and Zhu Y 2001 *Opt. Lett.* **26** 548
[48] Barzanjeh S and Vitali D 2016 *Phys. Rev. A* **93** 033846
[49] Xu X W, Liu Y, Sun C P and Li Y 2015 *Phys. Rev. A* **92** 013852
[50] Santos E G, Ramos D, Pini V, Calleja M and Tamayo J 2011 *Appl. Phys. Lett.* **98** 123108
[51] Luo G, Zhang Z Z, Deng G W, Li H O, Cao G, Xiao M, Guo G C, Tian L and Guo G P 2018 *Nat. Commun.* **9** 383
[52] Karabalin R B, Cross M C and Roukes M L 2009 *Phys. Rev. B* **79** 165309
[53] Huang P, Wang P F, Zhou J W, Wang Z X, Ju C Y, Wang Z M, Yang S, Duan C K and Du J F 2013 *Nat. Phys.* **9** 480
[54] Okamoto H, Gourgout A, Chang C Y, Onomitsu K, Mahboob I, Chang E Y and Yamaguchi H 2013 *Nat. (London)* **472** 69
[55] Zou C L, Han X, Jiang L and Tang H X 2016 *Phys. Rev. A* **94** 013812
[56] Han X, Zou C L and Tang H X 2016 *Phys. Rev. Lett.* **117** 123603
[57] Cleland A N and Geller M R 2004 *Phys. Rev. Lett.* **93** 070501
[58] Oaarconnell A D, Hofheinz M, Ansmann M, Bialczak R C, Lenander M, Lucero E, Neeley M, Sank D, Wang H and Weides M 2010 *Nature* **464** 697
[59] Xu X W and Li Y 2015 *Phys. Rev. A* **92** 69
[60] Si L G, Xiong H, Zubairy M S and Wu Y 2017 *Phys. Rev. A* **95** 033803
[61] Ma J, You C, Si L G, Xiong H, Li J, Yang X and Wu Y 2015 *Sci. Rep.* **5** 11278
[62] Barzanjeh S, Vitali D, Tombesi P and Milburn G J 2011 *Phys. Rev. A* **84** 042342
[63] Huang S and Agarwal G S 2011 *Phys. Rev. A* **83** 023823
[64] Cleland A 2009 *Nat. Phys.* **5** 458
[65] Alotaibi H M M and Sanders B C 2014 *Phys. Rev. A* **89** 021802
[66] Simon G, Klemens H, Vanner M R and Markus A 2009 *Nat. (London)* **460** 724
[67] Yan M, Rickey E G and Zhu Y 2001 *Phys. Rev. A* **64** 041801
[68] Li S, Yang X, Cao X, Zhang C, Xie C and Wang H 2008 *Phys. Rev. Lett.* **101** 073602
[69] Balic V, Braje D A, Kolchin P, Yin G Y and Harris S E 2005 *Phys. Rev. Lett.* **94** 183601
[70] Kumar P and Dasgupta S 2016 *Phys. Rev. A* **94** 023851
[71] Harris S E and Hau L V 1999 *Phys. Rev. Lett.* **82** 4611